



Research Paper

Altered glucose metabolism and cell function in keloid fibroblasts under hypoxia

Qifei Wang, Pu Wang, Zelian Qin^{*}, Xin Yang, Bailin Pan, Fangfei Nie, Hongsen Bi^{**}

Department of Plastic Surgery, Peking University Third Hospital, 49 North Garden Road, Haidian District, Beijing, China

ARTICLE INFO

Keywords:

Keloid
Fibroblasts
Cell metabolism
Hypoxia
Redox homeostasis
Autophagy

ABSTRACT

Keloids exhibit metabolic reprogramming including enhanced glycolysis and attenuated oxidative phosphorylation. Hypoxia induces a series of protective responses in mammalian cells. However, the metabolic phenotype of keloid fibroblasts under hypoxic conditions remains to be elucidated. The present study aimed to investigate glycolytic activity, mitochondrial function and morphology, and the HIF1 α and PI3K/AKT signaling pathways in keloid fibroblasts (KFB) under hypoxic conditions. Our results showed that hypoxia promoted proliferation, migration invasion and collagen synthesis and inhibited apoptosis in KFB. The mRNA levels, protein expressions and enzyme activities of glycolytic enzymes in KFB were higher than those in normal skin fibroblasts (NFB) under normoxia. Moreover, hypoxia remarkably upregulated glycolysis in KFB. Decreased activities of mitochondrial complexes and abnormal mitochondria were detected in KFB under normoxic conditions and the damage was aggravated by hypoxia. An intracellular metabolic profile assay suggested hypoxia increased glycolytic parameters except glycolytic reserve but inhibited the key parameters of mitochondrial function apart from H⁺ leak. Protein levels of HIF1 α and phosphorylation levels of the PI3K/AKT signaling pathway were upregulated in the context of 3% oxygen. Enhanced total reactive oxygen species (ROS), mitochondrial ROS (mitoROS) and antioxidant activities of KFB were observed in response to hypoxia. Additionally, autophagy was induced by hypoxia. Our data collectively demonstrated potentiated glycolysis and attenuated mitochondrial function under hypoxia, indicating that altered glucose metabolism regulated by hypoxia could be a therapeutic target for keloids.

1. Introduction

Keloids are disfiguring fibroproliferative disorders characterized by increased proliferation of fibroblasts and excessive deposition of extracellular matrix (ECM) [1]. Generally, keloids are abnormal healing conditions of wounds that frequently result from burns, trauma and infection. Clinically, keloids tend to grow beyond the original wound boundary and invade adjacent normal skin. They are clinically characterized by pain, itching and cosmetic deformities, and can be accompanied by ulceration, bleeding, and infection that severely affect quality of life. Although multiple therapies, such as surgical removal, glucocorticoid injections, laser therapy, and radiotherapy are available for keloids, the treatments are not satisfactory, and they cannot prevent recurrence [2]. In recent decades, genetics, inflammation and immune cells have been proven to be involved in the pathogenesis of keloids [3–5]. However, the mechanisms involved in keloid scarring are poorly understood, and keloids remain one of the most challenging skin

problems.

The Warburg effect (also referred to as aerobic glycolysis) is a metabolic phenotype detected in cancer cells in which glucose is employed to provide ATP through glycolysis rather than other oxidative phosphorylation in the presence of ample oxygen [6]. The altered metabolism fuels tumor growth by providing substrates for macromolecule synthesis, regulating apoptosis and maintaining redox status. The Warburg effect was first discovered in cancer cells. However, accumulating studies in recent decades have demonstrated that it exists in various types of cells and a variety of diseases. For instance, altered metabolism is observed in immune cells [7], LPS-activated macrophages [8], pulmonary hypertension [9], sepsis [10] and metabolic disorders [11]. Additionally, several studies reported that keloid is an aberrant scarring featuring metabolic reprogramming from oxidative phosphorylation to aerobic glycolysis [12,13]. Annette reported that compared to normal fibroblasts (NFB), cultured KFB exhibit increased glucose uptake and lactate accumulation and higher hexokinase,

^{*} Corresponding author.

^{**} Corresponding author.

E-mail addresses: qinzi@bjmu.edu.cn (Z. Qin), bihongsen@bjmu.edu.cn (H. Bi).

glyceraldehyde-3-phosphate dehydrogenase, and lactate dehydrogenase activities [12]. Vinaik [13] demonstrated the upregulation of GLUT1 and enhanced expression of several glycolytic enzymes such as HK1, HK2, PFK1, PFK2, PDK1 and PKM2 in keloid tissues compared with normal skin tissues. Our previous studies [14,15] indicated that KFB exhibit increased glycolysis and compromised mitochondrial functions. In addition to enhanced glucose consumption, lactate production and activities of glycolytic enzymes, we found that KFB are also characterized by higher basic glycolysis and glycolytic capacity and reduced basal oxidative respiration, maximal oxidative respiration and spare respiratory capacity.

Tissue hypoxia, a consequence of an insufficient oxygen supply caused by disordered vasculature and rapid growth of tumors, is found in various solid tumors and is clinically associated with therapy resistance and poor prognosis. Excessive collagen deposition and partially or completely occluded microvessels have been hypothesized to result in a hypoxic microenvironment within keloids. Okuno et al. [16] demonstrated that hypoxia exists in the keloid center and the hypoxic zone showed higher expression of HIF-1 α using immunohistochemical analysis. Importantly, hypoxia is considered a key mechanism of keloid formation. Our previous study showed increased proliferation, migration, invasion and collagen synthesis in KFB under hypoxia [17]. In addition, hypoxic conditions promote EMT [18] and inhibit apoptosis [19] in keloid fibroblasts. The lack of oxygen is linked to diseases such as cancer, diabetes, or inflammation but also constitutes a challenge for people living at high altitudes. Cells within organisms adapt to hypoxia by altering their metabolism. Accumulating studies have demonstrated hypoxia could significantly affect metabolic phenotype in cancer cells [20,21]. The association of hypoxia or HIF- α with altered metabolism in cardiovascular [22,23] and fibrotic disorders [24] was also reported. Many studies demonstrated that chronic hypoxia triggers signaling pathways that regulate cardiac metabolic remodeling, particularly at the transcriptional level, to maintain energy production. He et al. reported elevated HIF-1 α expression and altered endothelial metabolism, including increased glycolysis and reduced oxygen consumption in the endothelium of coronary arteries after mice were treated with a PHD inhibitor, dimethylxalylglycine. Gopu et al. [25] observed increased basal expression of HIF-1 α and glycolytic enzymes as well as lactate and succinate levels in fibrotic lung fibroblasts compared with normal lung fibroblasts. Keloids typically feature excessive proliferation of fibroblasts and deposition of ECM and microvascular abnormalities. Collectively, KFB may undergo similar metabolic reprogramming in hypoxia. However, alteration in KFB metabolism under hypoxia is rarely investigated. Hence, we postulated that hypoxia triggers metabolic reprogramming to regulate cell functions.

It has been demonstrated that KFB exhibit metabolic reprogramming [12,14]. More importantly, hypoxia can regulate energetic metabolism in a majority of cancer cells [20]. Hence, the present study aimed to evaluate the glycolytic activity and mitochondrial function of KFB under hypoxia and to elucidate the potential mechanism. In addition, redox homeostasis and autophagy levels in hypoxia were also analyzed.

2. Materials and methods

2.1. Isolation and culture of fibroblasts

Normal skin tissues and keloid samples were obtained from individuals who underwent surgery. None of them received clinical therapy to prevent scar development prior to surgery. Basic information of species is presented in [Supplementary Table S1](#). Isolation and culture of fibroblasts were performed as reported previously with minor modifications [1]. Specimens were dissected into 1 mm³ piece and digested with 0.1% collagenase I (Sigma-Aldrich, USA) in a constant temperature shaker at 37 °C for 2 h. The digested suspension was filtered and centrifuged. The pellets were cultured in Dulbecco's Modified Eagle's medium (DMEM) (HyClone, USA) with 10% fetal bovine serum (Gibco,

USA) and 1% penicillin/streptomycin (HyClone, USA). When reaching approximately 80% confluence, the 4 to 6 passages of fibroblasts were used for the experiments. The study was approved by the ethics committee of Peking University Third Hospital and followed the principles documented in the Declaration of Helsinki. Written informed consent was provided by all participants.

2.2. Oxygen concentration determination and proliferation assays

To determine the optimal oxygen level promoting KFB proliferation, KFB were cultured in incubators with different O₂ levels. Briefly, 1.2×10^5 cells were seeded into 6-well culture plates and cultured in incubators with 1%, 2%, 3%, 4%, 5% and 21% O₂ concentrations for 48 h. Cells were collected with 0.25% trypsin (HyClone, USA). The total number of cells was determined by cell counting under a microscope (Leica, Germany). Additionally, we investigated the effect of hypoxia (3%) on the proliferation of NFB and KFB. A total of 1.2×10^5 cells were seeded into 6-well plates and incubated for 24, 48 and 72 h with 3% or 21% O₂. Cells were harvested and the total number was counted by a microscopy.

2.3. Measurement of intracellular ROS and mitoROS

ROS and mitoROS were measured with a Reactive Oxygen Species Assay Kit (Beyotime, China) and MitoSOX Red reagent (Invitrogen, USA), respectively. Briefly, 2×10^5 cells/per well were seeded into 6-well plates and cultured in incubators containing 3% or 21% O₂ at 37 °C for 24 h. For ROS assays, cells were collected and incubated in 10 μ M DCFH-DA working solution for 20 min at 37 °C in the dark. For mitoROS determination, cells were incubated in 1 ml of 5 μ M MitoSOX reagent working solution at 37 °C. After incubation, cells were washed twice with serum-free medium to remove working solution that did not enter cells. Finally, the fluorescence intensity was detected by a flow cytometer (BD, USA).

2.4. Apoptosis analysis

Cell apoptosis was investigated using an Annexin V-PE/7-AAD apoptosis detection kit (KeyGEN, China) with flow cytometry according to the manufacturer's instruction. Briefly, fibroblasts were initially seeded in 6-well plates at a density of 1.5×10^5 cells/well. After incubated in chambers with 3% or 21% O₂ levels for 48 h, cells were harvested and resuspended in 500 μ l binding buffer. Then 5 μ l Annexin V-PE and 5 μ l 7-AAD were added to the above solution. The apoptosis results were detected by flow cytometry (BD, USA).

2.5. Migration and invasion assay

Migration assays were conducted using a transwell chamber with 8.0 μ m pores (Corning, USA). Briefly, 1×10^4 cells were resuspended in the upper compartment of the chamber with 200 μ l serum-free medium and 500 μ l complete medium were added into the lower compartment. After incubation for 24 h at normoxic or hypoxic conditions, the upper cells were removed with swabs. The migrated cells were fixed with 4% paraformaldehyde for 20 min and stained with 0.1% crystal violet for 20 min. The number of migrating cells was counted in 5 randomly chosen fields under the microscope (100 magnification) and the mean of each chamber was calculated.

Invasion assays were slightly different from migration assays. Matrigel was diluted with DMEM as the volume ratio of 1–8. 40 μ l diluted matrigel was uploaded in the upper compartment and then the transwell chambers were placed in incubators for 2 h. 2×10^4 cells were seeded into the upper compartment of the chamber and were conditioned in incubators with 3% or 21% O₂ for 36 h. Other processes were similar to migration assays.

2.6. Glucose consumption and lactate production

Glucose consumption and lactate production were measured using a glucose assay kit (Solarbio, China) and lactate assay kit (Solarbio, China), respectively. In brief, cells were seeded into 96-well plates at a density of 4000 cells/well in 100 μ l DMEM. After incubation at 37 °C for 4 h, the culture medium was replaced and cells were incubated for 24 h under 21% or 3% O₂. The supernatant was collected for the detection of glucose intake and lactate accumulation according to the manufacture instructions. The absorbances at 505 nm and at 450 nm were recorded on a microplate reader (Thermo Fisher Scientific, USA) for glucose consumption and lactate production, respectively.

2.7. Activities of NADPH oxidase (NOX), antioxidant enzymes, glycolytic enzymes and mitochondrial complexes

Activities of NOX, superoxide dismutase (SOD), glutathione peroxidase (GSH-Px), PKM2, LDHA, HK2 and PFKFB3 activities were detected by the corresponding enzyme activity kit (Solarbio, China). Besides, PGK1 and ENO1 activities were determined by a commercial kit provided by comin biotechnology (Suzhou, China) and Abnova (Paipai, China), respectively. Mitochondrial complexes I-IV activities were determined using mitochondrial respiratory chain complex activity detection kits (Solarbio, China). Briefly, after fibroblasts were cultured at normoxia or hypoxia (3%), cells were collected and lysed with extracting solution (1ml/10⁶ cells). For activities of NOX, antioxidant enzymes and glycolytic enzymes, the cells were broken by the ultrasonic wave and centrifuged, and the supernatant was placed on ice for a test. For measurement of mitochondrial complexes activities, mitochondrial extraction was performed according to the manufacturer's instructions and the mitochondrial extract was employed for measurements of complex activities and determinations of protein concentrations. The absorbance was measured by a microplate reader at 600 nm for NOX, 560 nm for SOD, 412 nm for GSH-Px, 340 nm for PKM2, 450 nm for LDHA, 340 nm for HK, 340 nm for PFKFB3, 340 nm for PGK1, 570 nm for ENO1, 340 nm for Complex I, 605 nm for Complex II or 550 nm for Complex III and complex IV, respectively. The calculations of the enzyme activities were based on the formula presented in the specification. NOX, SOD and GSH-Px activities were presented as U/mg prot. Glycolytic enzyme activities were expressed as nmol/min/10⁴ cells. Mitochondrial complex activity was expressed as nmol/min/mg prot.

2.8. RNA extraction and qRT-PCR

Total RNA was isolated from collected cells with Trizol reagent (Invitrogen, USA). The quantity of extracted RNA was performed with the Nanodrop 2000 spectrophotometer (Thermo Fisher Scientific, USA). cDNA synthesis was accomplished using the FastKing RT Kit (with gDNase) (Tiangen Biotech, China). qRT-PCR was performed in line with the Talent qPCR PreMix (SYBR Green) kit protocol (Tiangen Biotech, China) using an ABI Quant- Studio 5 Real-Time PCR System (Applied Biosystems, USA). Relative quantifications and calculations were completed using the 2^{- $\Delta\Delta$ CT} method. Primer sequences are presented in [Supplementary Table S2](#).

2.9. Western blotting

Cells were lysed in RIPA lysis buffer (Solarbio, China) supplemented with phosphatase and protease inhibitor cocktail (Solarbio, China). The cell lysates were centrifuged and protein concentrations were determined using a BCA Protein Assay kit (Beyotime, China). 30 μ g protein samples were separated by 10% SDS-PAGE and transferred to PVDF membranes with 0.45 μ m of pores (Millipore, MA, USA). Membranes were blocked with 5% non-fat dry milk for 1 h, followed by incubation overnight at 4 °C with primary antibodies ([Supplementary Table S3](#)). The membranes were then washed and incubated with HRP conjugated

secondary antibody, washed with Tris-buffered saline (TBS) and Tween 20 (0.1%) (TBST). The western blotting bands were visualized by using an enhanced chemiluminescence system (Amersham Pharmacia Biotech, United Kingdom). Densitometric analysis was performed with Image J software.

2.10. Mitochondrial mass and mitochondrial membrane potential (MMP) measurement

Mitochondrial mass and MMP were determined using Mito-Tracker Green (Beyotime, China) and JC-1 (Beyotime, China), respectively. Briefly described, after 1.5 \times 10⁵ cells were seeded into 6-well plates and were cultured at normoxia or hypoxia for 48 h for mitochondrial mass or for 24 h for MMP, cells were collected and centrifuged. For Mitochondrial mass determination, cells were incubated with prewarmed 200 nM MitoTracker Green staining solution at 37 °C in the dark for 15 min. For MMP measurement, cells were stained with 500 μ l 10 μ g/ml JC-1 for 20 min at room temperature in darkness. And then cells were resuspended in 500 μ l serum-free DMEM. The fluorescence intensity was detected by flow cytometer. Green fluorescence intensities documented for mitochondrial mass, and red and green fluorescence intensities were analyzed for MMP.

2.11. Extracellular acidification rate (ECAR) and oxygen consumption rate (OCR) measurement

Glycolysis and mitochondrial oxidative phosphorylation were evaluated by the ECAR and OCR using The XF96 Extracellular Flux Analyzer (Seahorse Bioscience, USA). Briefly, 1 \times 10⁴ cells/well were seeded into a special 96-well plate and incubated under normoxia or hypoxia (3%) for 24 h. Sensor cartridges were treated with XF calibrant (200 μ l/well) for 24 h at 37 °C in a humidified incubator without CO₂. Cells were washed twice with the Seahorse XF stress test assay medium and the final volume was 175 μ l/well. The injections in ECAR and OCR measurement were glucose (10 mM), oligomycin (2 μ M), 2-DG (50 mM) and oligomycin (2 μ M), FCCP (2 μ M), rotenone/antimycin A (1 μ M), respectively. Data were normalized to total protein content using a BCA assay. ECAR in mpH/min/prot and OCR is reported in pmol/min/ug prot.

2.12. Evaluation of autophagic cells

Cells were transfected with mRFP-GFP-LC3B (HanHeng, China) with MOI 300 for 8 h in the light of the manufacturer's protocol, and then the media were exchanged for fresh complete media, cultured for additional 40 h. Cells were cultured under normoxia or hypoxia (3%) for 24 h and imaged using confocal fluorescence microscopy. The number of GFP and RFP dots was identified by manual counting of fluorescence puncta.

2.13. Transmission electron microscope imaging

Electron microscopy was employed to morphologically observe autophagy and mitochondria. Cells were collected and fixed with 2.5% ice-cold glutaraldehyde and post fixed in 1% osmium tetroxide for 2 h at 4 °C. After dehydration in a series of ethanol gradients, the cells were embedded in epoxy resin and polymerized at 60 °C, cut into 50 nm sections and further stained with 3% uranyl acetate and lead citrate. Six random fields of each sample were observed under a transmission electron microscope (TEM) (JEM1400 plus, Japan).

2.14. Statistical analysis

Data in the study are expressed as the mean \pm standard deviation. The Kolmogorov-Smirnov and Levene tests were used to investigate normal distribution and homogeneity of variance, respectively. Student's t-test was performed to analyze differences between two groups,

and one-way ANOVA or two-way ANOVA was used to analyze intergroup differences with a Bonferroni multiple comparison post-test. Statistical analyses were performed using the SPSS 26.0 software. A *P* value < 0.05 was considered to be statistically significant. Experiment data represent at least three independent experiments.

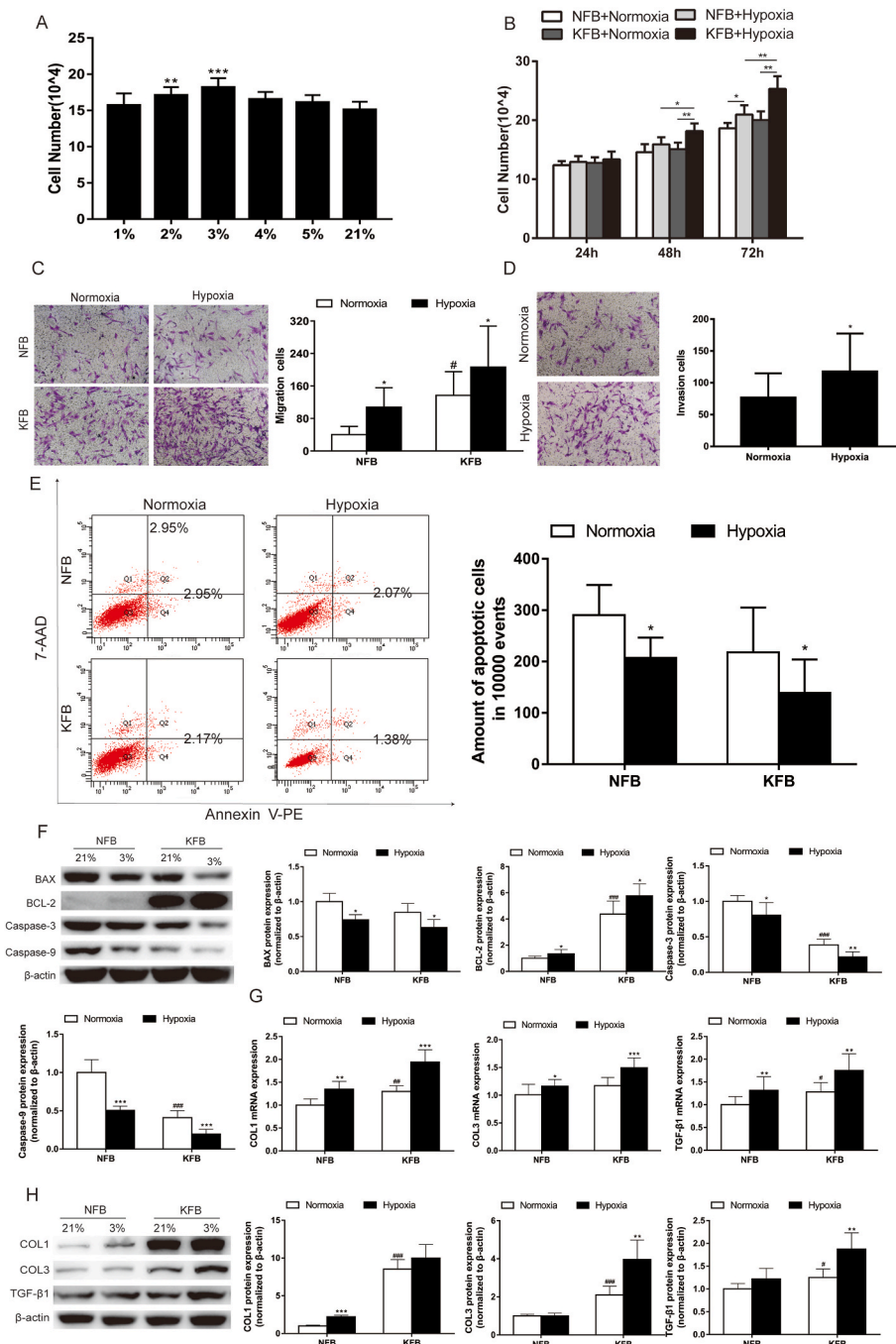
3. Results

3.1. Hypoxia (3%) promoted proliferation, migration, invasion and collagen synthesis and inhibited apoptosis

Hypoxia is a common phenomenon in a series of solid tumors, and it can significantly affect the tumor microenvironment. To explore the effect of hypoxia on cell characteristics, including proliferation, migration, invasion and apoptosis, we first determined the optimal O₂ level

using a proliferation assay. The findings indicated that the 3% O₂ level had a more proliferative effect than other oxygen concentrations (Fig. 1A). Accordingly, the 3% O₂ level was adopted in the following experiments. When KFB and NFB were cultured at 3% and 21% oxygen concentrations for 24, 48 and 72 h, KFB exhibited higher proliferation rate than NFB both under normoxia and hypoxia. Hypoxia (3%) presented an obvious proliferative effect compared to normoxia (Fig. 1B). Migration and invasion are critical properties of tumors. Hence, we investigated the migration and invasion feature of KFB under hypoxia. The results suggested that hypoxia (3%) promoted migration (Fig. 1C) and invasion (Fig. 1D). In normoxic conditions, KFB presented decreased apoptosis compared to NFB, and hypoxia inhibited apoptosis in KFB and NFB (Fig. 1E). At the same time, western blotting showed that caspase-3 and caspase-9 expression was markedly decreased in KFB cultured under hypoxia for 48 h (Fig. 1F). Keloids are characterized by excessive

Fig. 1. The effect of hypoxia (3%) on proliferation, migration, invasion, apoptosis and collagen synthesis in KFB and NFB. (A) Hypoxic conditions promote proliferation in KFB. KFB were exposure to different oxygen levels (1%, 2%, 3%, 4%, 5% and 21% O₂) for 48 h in a hypoxia chamber. Cells numbers were counted under microscopy. Data are presented as Mean ± S.D.(n = 6). ***P* < 0.01, ****P* < 0.001 versus 21%. (B) Hypoxia (3%) promotes proliferation in KFB and NFB. KFB and NFB were conditioned at 3% and 21% oxygen concentrations for 24, 48 and 72 h. Effect of hypoxia on proliferation in KFB and NFB was assessed by cell counting using microscopy. Hypoxia (3%) enhanced migration (C) and invasion (D) in KFB and NFB, as explored by transwell assays. (E) Hypoxia (3%) inhibited apoptosis in KFB and NFB demonstrated by flow cytometric analyses. (F) Decreased mitochondrial apoptosis pathways including BCL-2, BAX, Caspase-3 and Caspase-9 were detected using western blotting. Hypoxia (3%) enhanced mRNA (G) and protein (H) levels of collagens production in KFB and NFB. Data are presented as Mean ± S.D.(n = 6). #*P* < 0.05, ##*P* < 0.01, ###*P* < 0.001 versus NFB under normoxia. **P* < 0.05, ***P* < 0.01, ****P* < 0.001 versus represent NFB or KFB in hypoxia versus that under normoxic conditions.



deposition of the extracellular matrix. Collagen I and collagen III expression in KFB and NFB was analyzed by qRT-PCR and western blotting. The results showed they were significantly upregulated under hypoxia (Fig. 1G and H).

3.2. Elevated levels of ROS and mitoROS under hypoxic conditions

Redox balance is crucial to cell physiology and hypoxia can impair redox homeostasis. While ROS biology under hypoxia has been studied extensively, it remains inconsistent whether ROS levels decrease or increase at prolonged low oxygen. In the present study, we investigated ROS levels in KFB and NFB under hypoxia (3%). When cells were cultured in normoxia, ROS (Fig. 2A) and mitoROS (Fig. 2B) levels in KFB were higher than that in NFB. Moreover, their generations were enhanced under hypoxia. To elucidate the regulatory mechanism of ROS under hypoxia, NOX activity and the activity of antioxidant enzymes were investigated. Interestingly, NOX (Fig. 2C), SOD (Fig. 2D), and GSH-Px (Fig. 2E) activities were enhanced under hypoxia.

3.3. Glucose intake and lactate production increased in the context of 3% O₂

Our previous study suggested that keloids underwent metabolic reprogramming of aerobic glycolysis featuring enhanced glucose intake and lactate production under normoxic conditions. However, glucose consumption and lactate accumulation in KFB have not been

investigated under hypoxia before. In the study, KFB and NFB were incubated in hypoxia (3%) or normoxia for 24 h, glucose consumption (Fig. 3A) and lactate accumulation (Fig. 3B) under hypoxia were remarkably higher than in the context of normoxia. Moreover, hypoxia significantly increased HK (Fig. 3C) and LDH (Fig. 3D) activities. Additionally, the mRNA level (Fig. 3E and F) and protein expression (Fig. 3G–I) of GLUT1 and LDHA under hypoxia were more elevated than that under normoxia. Furthermore, LDHA activity in hypoxia increased compared to that under normoxic conditions.

3.4. Hypoxia (3%) enhanced mRNA expression, protein level and activities of glycolytic enzymes

Our previous work showed that cellular metabolism in keloids is markedly different from that of normal skin. KFB have increased rates of glycolysis under normoxic conditions. However, the metabolic phenotype of KFB in hypoxia remains to be elucidated. To evaluate glycolysis of KFB under low oxygen conditions, the mRNA expression, protein level and activities of key glycolytic enzymes including PGK1, ENO1, PKM2, PFKFB3 and HK2 were investigated. The mRNA levels (Fig. 4A–E) of glycolytic enzymes in KFB increased when cells were cultured in hypoxia for 12 h. In addition, hypoxia for 24 h did potentiated protein expression (Fig. 4G–K) and activity (Fig. 4L–O). In brief, KFB augmented glycolysis to adapt to the hypoxic microenvironment.

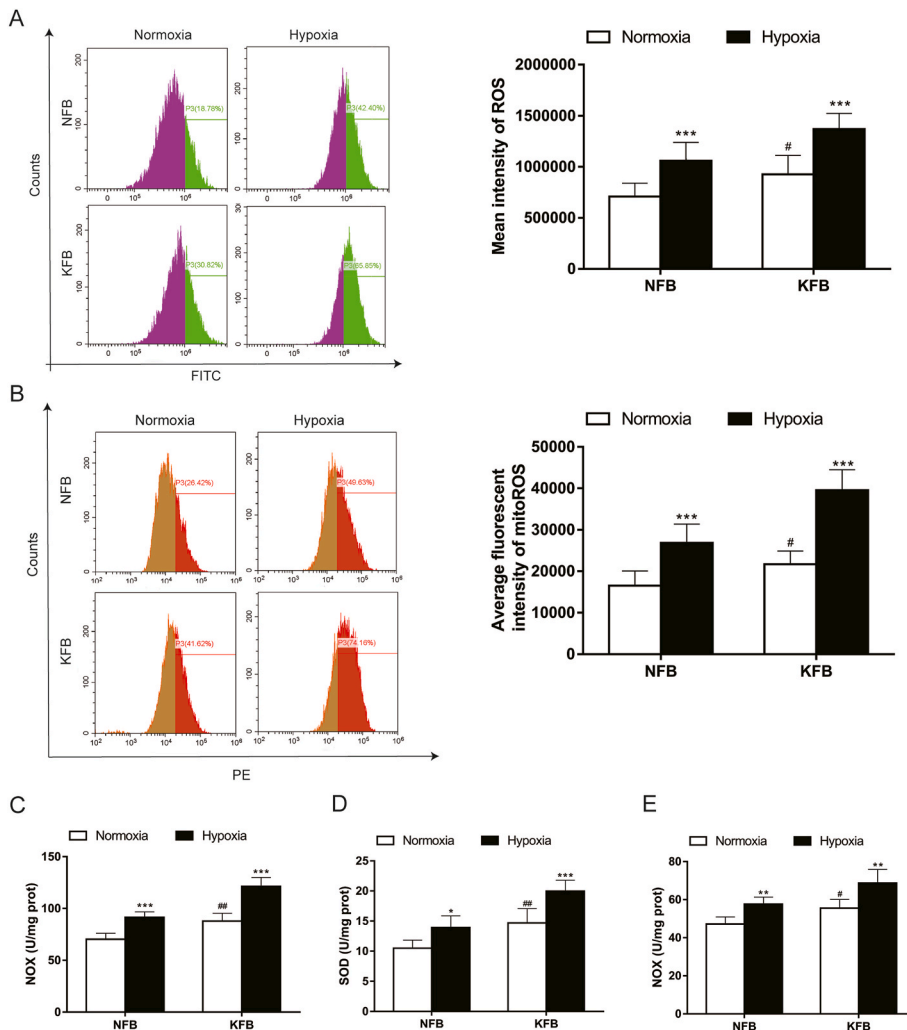


Fig. 2. Redox balance under hypoxia (3%) in KFB and NFB. Flow cytometry for the detection of ROS intensity (A) and mitoROS intensity (B) in KFB and NFB. Hypoxia (3%) enhanced production of ROS and mitoROS in KFB and NFB. NOX (C), SOD (D) and GSH-Px (E) activities were evaluated. Hypoxia significantly increased the above enzymes activities. Data are presented as Mean \pm S.D.(n = 6). #P < 0.05, ##P < 0.01, ###P < 0.001 versus NFB under normoxia. *P < 0.05, **P < 0.01, ***P < 0.001 versus represent NFB or KFB in hypoxia versus that under normoxic conditions.

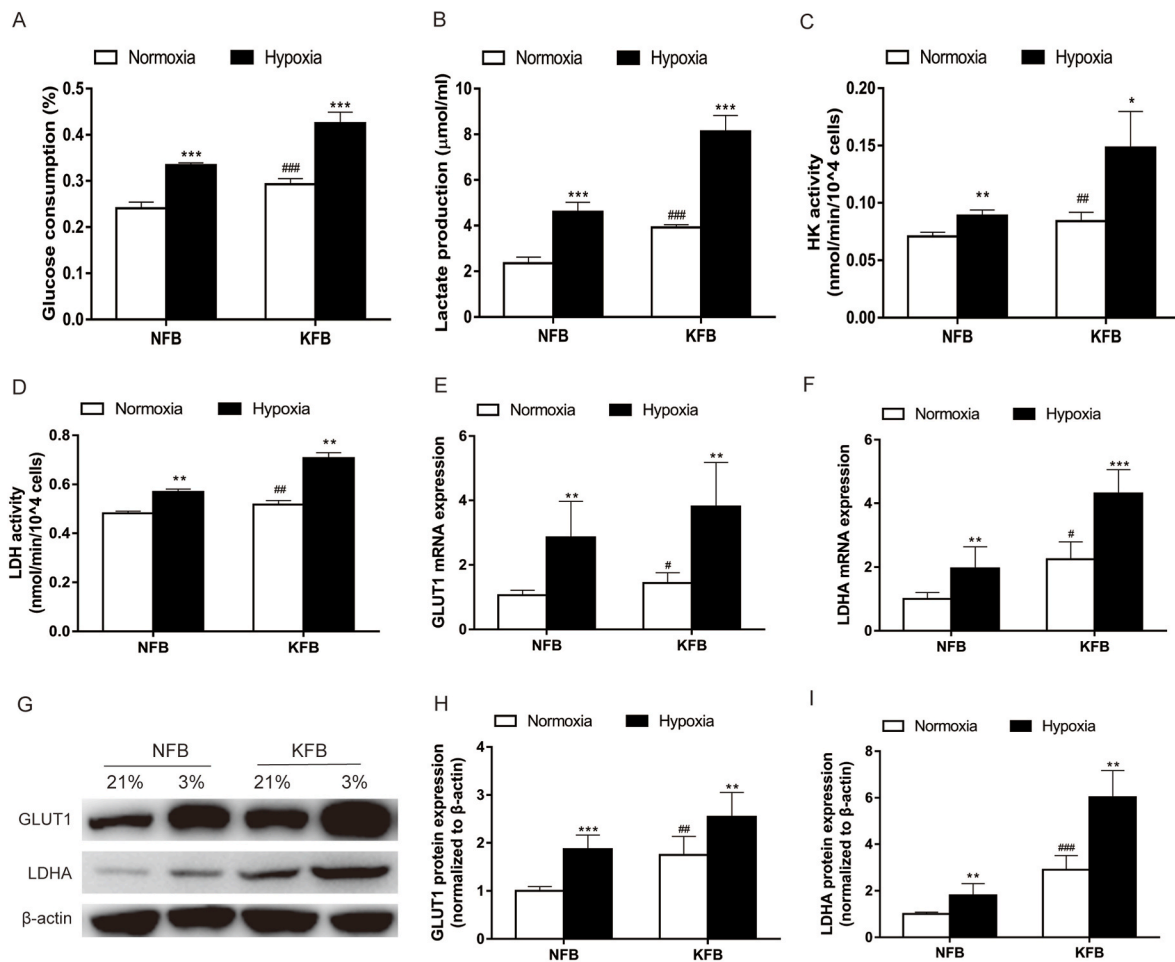


Fig. 3. Glucose consumption and lactate production in KFB and NFB increased under hypoxia (3%) compared with normoxia. (A) Glucose consumption. (B) Lactate production. (C) HK activity. (D) LDH activity. The mRNA (E–F) and protein (G–I) levels of GLUT1 and LDHA were determined. Data are presented as Mean \pm S.D. (n = 6). *P < 0.05, **P < 0.01, ***P < 0.001 versus NFB under normoxia. #P < 0.05, ##P < 0.01, ###P < 0.001 versus represent NFB or KFB in hypoxia versus that under normoxic conditions.

3.5. Alteration of mitochondrial functions and ultrastructure under hypoxia

Mitochondria are crucial for energy metabolism and apoptosis regulation. Mitochondria in keloids undergo specific alterations to survive and grow under hypoxic conditions. Hypoxia can significantly affect mitochondrial biogenesis and membrane potential. In this study, the mitochondrial mass increased after hypoxia for 48 h, investigated by a mitochondrial green explorer (Fig. 5A). Hence, KFB can provide more ATP by augmenting mitochondrial biogenesis even in at low oxygen levels. Membrane potential reflects the health state of mitochondria. Mitochondrial membrane potential decreased at an early period of apoptosis. We observed that membrane potential increased in KFB and NFB after hypoxic culture for 24 h (Fig. 5B), which can protect cells from apoptosis. Mitochondrial complexes I–IV are indispensable for cellular respiration. Moreover, dysfunctions of complex I–III are responsible for mitoROS production. The activities of complexes I–IV were investigated in this study (Fig. 5C). Complexes activities in KFB decreased compare to that in NFB in normoxic condition. Furthermore, complex activities in KFB and NFB were compromised under hypoxia. Mitochondrial ultrastructure is intimately linked to cellular bioenergetic status. Finally, we observed mitochondrial morphology using transmission electron microscopy (TEM). In normoxic conditions, mitochondria in NFB presented bilayer membrane ultrastructure and wrinkled cristae (Fig. 5D). However, KFB feature swollen mitochondria, cristae effacement and vacuolization. When NFB and KFB were incubated in hypoxia, we

observed increased mitochondrial damage in KFB (Fig. 5D).

3.6. Hypoxia (3%) increased ECAR and attenuated OCR

Glycolysis and oxidative phosphorylation are the two major sources of energy in the cell. The XF instrument can directly monitor the extracellular acidification rate (ECAR) and the oxygen consumption rate (OCR) in real time. The Seahorse XFp glycolysis stress test was carried out to assess glycolysis by the continuous adjunction of glucose, oligomycin and 2-DG. KFB exhibited higher key parameters of glycolytic flux than NFB: glycolysis, glycolytic capacity, glycolytic reserve, and non-glycolytic acidification in normoxic condition when compared to NFB (Fig. 6A and B). Furthermore, KFB and NFB presented enhanced non-glycolytic acidification (Fig. 6C), glycolysis (Fig. 6D) and glycolytic capacity (Fig. 6E), and decreased glycolytic reserve in hypoxia (Fig. 6F).

A Seahorse XFp cell mito stress test kit was performed to evaluate important parameters of oxidative phosphorylation by the consecutive addition of oligomycin, FCCP, and rotenone/antimycin A. Under normoxic conditions, KFB demonstrated attenuated ATP production, maximal respiration, spare respiratory capacity, nonmitochondrial respiration and coupling efficiency compared with NFB (Fig. 6G and H). Meanwhile, H^+ (Proton) leakage in KFB was higher than in NFB. When cells were cultured in hypoxia, H^+ leakage in KFB and NFB increased (Fig. 6N). However, other key parameters of OCR were hindered by hypoxia (Fig. 6I–M). Furthermore, the ratio of OCR/ECAR significantly decreased in KFs in normoxia (Fig. 6P), indicating a metabolic shift to

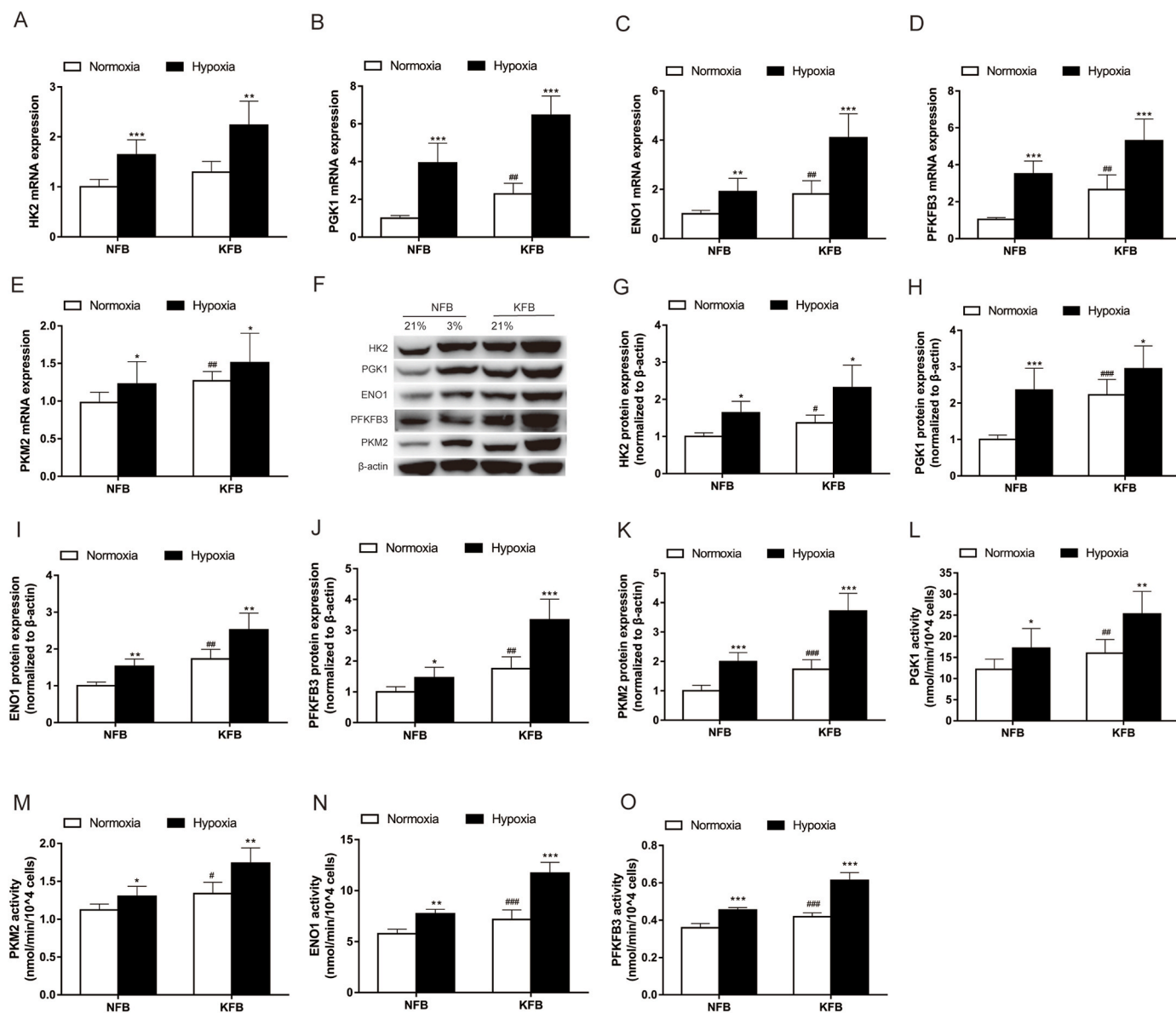


Fig. 4. Evaluation of mRNA expression, protein level and activities of glycolytic enzymes under hypoxia (3%) in KFB and NFB. (A–E) The mRNA levels of glycolytic enzymes were investigated by RT-PCR. mRNA was collected after cells culture for 12 h under hypoxia (3%) or normoxia. (F–K) The protein levels of glycolytic enzymes were determined by western blotting. Proteins were collected after cells incubation for 24 h under hypoxia (3%) or normoxia. (L–O) Activities of glycolytic enzymes were investigated using glycolytic enzyme activities kits. The evaluations were performed after cells incubation for 24 h under hypoxia (3%) or normoxia. Data are presented as Mean \pm S.D. (n = 6). #P < 0.05, ##P < 0.01, ###P < 0.001 versus NFB under normoxia. *P < 0.05, **P < 0.01, ***P < 0.001 versus represent NFB or KFB in hypoxia versus that under normoxic conditions.

aerobic glycolysis. In addition, hypoxia suppressed OCR/ECAR in KFB and NFB, suggesting that cells undergo metabolic programming in hypoxia.

3.7. Autophagy was enhanced under hypoxic conditions

Cells were cultured under hypoxia or normoxia for 24 h. Western blot analysis showed increased LC3-II/ β -actin level and decreased p62 protein level in KFB compared to NFB under normoxia (Fig. 7A–C). In addition, hypoxia promoted LC3-II/ β -actin levels and attenuated p62 levels in KFB and NFB (Fig. 7A–C). To further observe autophagy flux, cells were treated with tandem fluorescent mRFP-GFP-LC3. KFB exhibited more autophagosomes and autolysosomes than NFB in normal oxygen. After hypoxia exposure for 24 h, autophagosomes and autolysosomes significantly increased (Fig. 7D and E). ETM was also performed to morphologically observe the induction of autophagy in cells. Both

autophagosomes and autolysosomes markedly accumulated in cells after exposure to hypoxia (Fig. 7F).

3.8. HIF1 α and PI3K-AKT pathway was upregulated under hypoxia (3%)

HIF1 α regulates the expression of genes related to metabolism and adapts cells to the hypoxic microenvironment. The ubiquitous PI3K-AKT signaling pathway has diverse downstream effects on cellular metabolism via either direct regulation of metabolic enzymes and nutrient transporters or the control of transcription factors involved in the regulation of metabolic pathways. In this study, the effect of hypoxia on the regulation of HIF1 α and PI3K-AKT pathway was investigated by Western blot analysis. Western blotting did not detect the expression of HIF1 α in cells under normoxia. However, hypoxia remarkably increased the HIF1 α expression (Fig. 8A and B). What's more, the expression level in KFB was more notable than that in NFB in the context of hypoxia. In

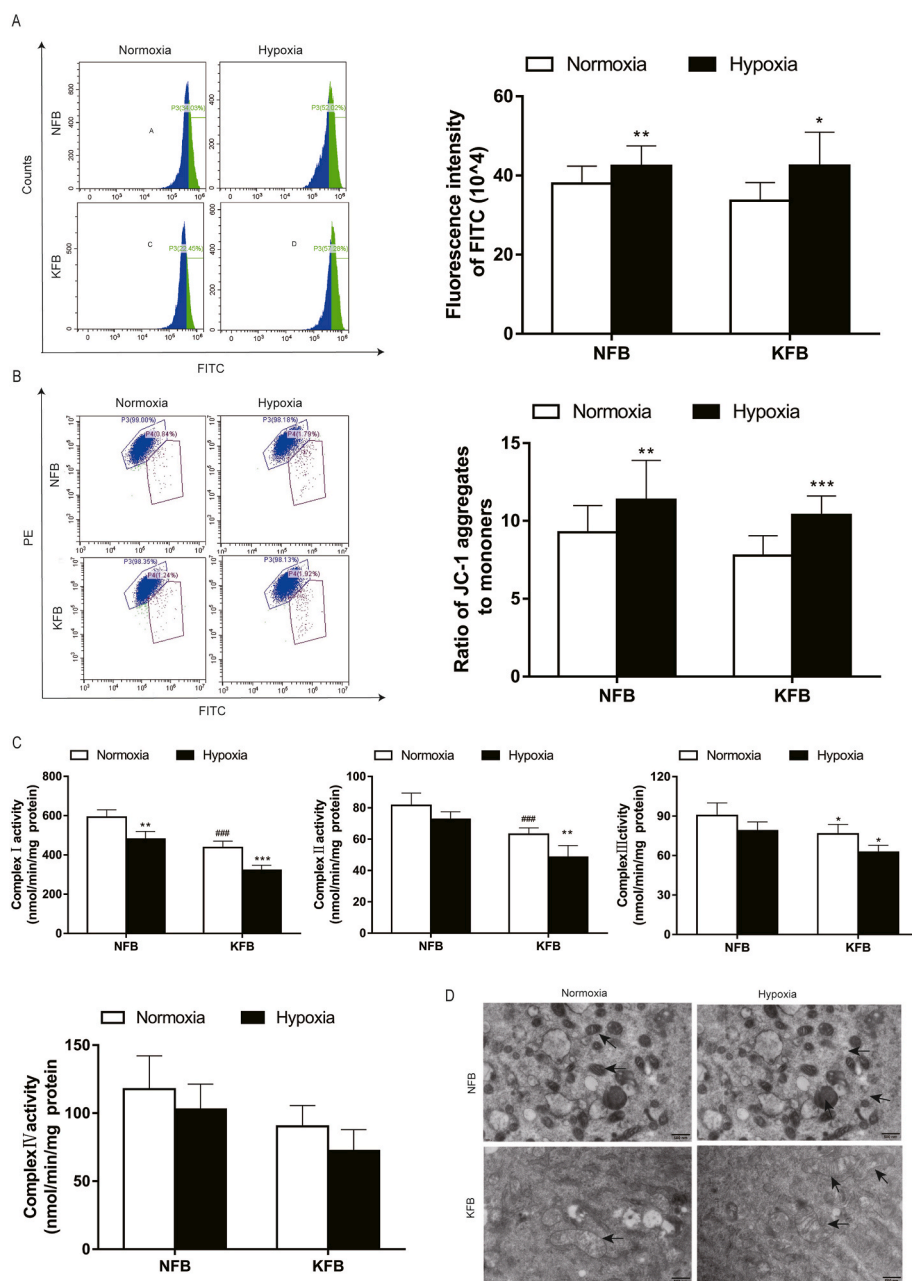


Fig. 5. Mitochondrial mass, membrane potential, mitochondrial complex activities and morphology in KFB and NFB under hypoxia (3%). (A) Hypoxia (3%) augmented mitochondrial mass in KFB and NFB after incubation for 48 h, determined with mitochondrial green explorer. (B) Mitochondrial membrane potential increased under hypoxia (3%) for 24 h, measured by flow cytometry. (C) Mitochondrial complex activities were inhibited after conditioned at 3% O₂ level for 24 h. (D) Mitochondrial ultrastructure is analyzed by TEM. Data are presented as Mean \pm S.D. (n = 6). #P < 0.05, ##P < 0.01, ###P < 0.001 versus NFB under normoxia. *P < 0.05, **P < 0.01, ***P < 0.001 versus represent NFB or KFB in hypoxia versus that under normoxic conditions. (For interpretation of the references to colour in this figure legend, the reader is referred to the Web version of this article.)

normoxic condition, there was no significant difference in the total levels of PI3K (Fig. 8C) and AKT (Fig. 8E) in KFB and NFB, while the phosphorylation levels of PI3K (Fig. 8D) and AKT (Fig. 8F) in KFB were enhanced compared with those of NFB. Additionally, hypoxia had no effect on the total levels of PI3K and AKT in either KFB or NFB. However, low oxygen levels promoted the phosphorylation levels of PI3K and AKT in both types of fibroblasts. Hence, hypoxia may mediate metabolism through the PI3K-AKT pathway.

4. Discussion

Our previous study demonstrated augmented glycolysis and impaired mitochondrial function in KFB. Additionally, mounting studies have shown that hypoxia is related to poor prognosis in patients with tumors and contributes to therapy resistance. However, the metabolic phenotype of KFB under hypoxia and the potential mechanism are poorly documented. In the present study, we evaluated glycolysis,

mitochondrial function and morphology as well as the involvement of HIF1 α and the PI3K/AKT signaling pathway in KFB at hypoxic conditions. Additionally, redox homeostasis and autophagy under hypoxia were also investigated.

Rapid proliferation and insufficient blood supply of solid tumors lead to diminished oxygen availability. Hypoxia significantly contributes to the cellular expression program and thereby promotes proliferation and regulates apoptosis. In this study, we first determined a 3% O₂ level as the optimal O₂ concentration using proliferation assay and the 3% O₂ level was adopted in the following assays. The proliferation rate of KFB was higher than that of NFB in normoxia. What's more, we observed that hypoxia can promote the proliferation of KFB and NFB. The proliferative effect of hypoxia on fibroblasts was also observed in other types of fibroblasts derived from lung [26] and artery [27]. Although studies on the effect of hypoxia on apoptosis in keloids have been conducted, conflicting results have been reported. Ladin et al. reported that hypoxic condition (\leq 2% oxygen) selectively induced apoptosis in keloid

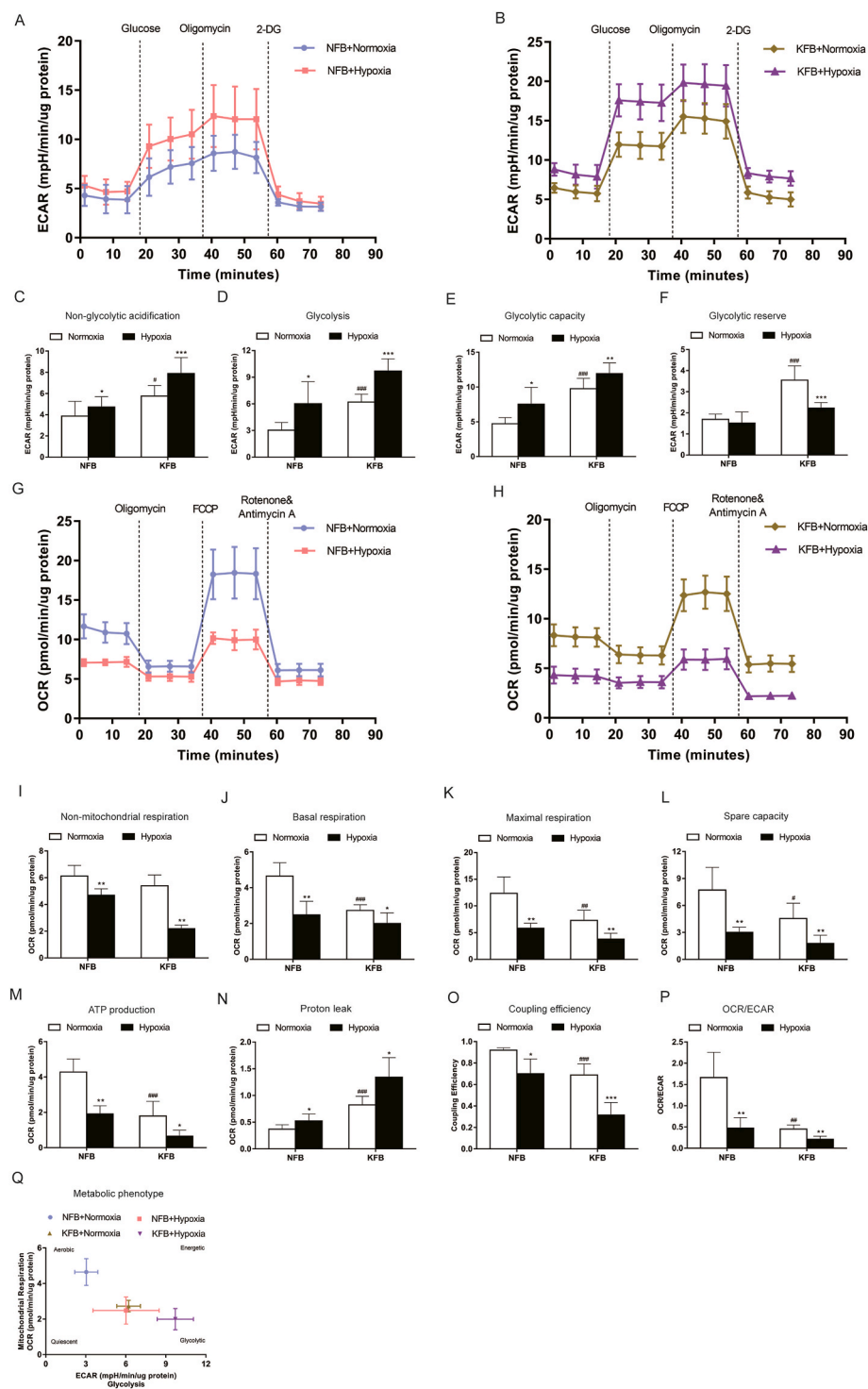


Fig. 6. Hypoxia (3%) promoted glycolytic activity and impaired mitochondrial function in KFB and NFB. Representative glycolytic stress tests were performed for NFB (A) and KFB (B) using a Seahorse Bioscience XF96 Extracellular Flux Analyzer. KFB and NFB cultured in the context of 3% O₂ showed increased non-glycolytic acidification (C), glycolysis (D), glycolytic capacity (E) and glycolytic reserve (F). Representative mitochondrial stress tests were conducted for NFB (G) and KFB (H). Hypoxia (3%) inhibited non-mitochondrial oxygen consumption (I), basal respiration (J), maximal respiration (K), spare respiratory capacity (L), ATP production (M), coupling efficiency (O), and increased proton leak (N). (P) OCR/ECAR ratio. (Q) Metabolic phenotype. Data are presented as Mean ± S.D. (n = 6). #P < 0.05, ##P < 0.01, ###P < 0.001 versus NFB under normoxia. *P < 0.05, **P < 0.01, ***P < 0.001 versus represent NFB or KFB in hypoxia versus that under normoxic conditions.

fibroblasts when compared with normal adult fibroblasts [28]. Lei and his colleagues found that the apoptotic number of keloid fibroblasts was stimulated by hypoxia (1%) but not significantly increased [29]. In our study, hypoxia (3%) inhibited apoptosis in KFB and NFB. To clarify the potential apoptosis mechanism of KFB in hypoxia, we evaluated the mitochondrial apoptosis pathway. Interestingly, decreased protein levels of BAX, caspase-3 and caspase-9 as well as potentiated BCL-2 expression were observed in hypoxia. It is postulated that the variation in oxygen levels may be responsible for the different effects of hypoxia on apoptosis. Extremely low oxygen promotes apoptosis but appropriate hypoxia inhibits cellular apoptosis and contributes to

survival.

Redox homeostasis is essential for maintaining physiological functions, while redox imbalance is viewed as a potentially oxidant damage and contributes to the pathological process. But it remains controversial whether hypoxia promotes or inhibits ROS generation. In the study, we evaluated ROS and mitoROS production in KFB and NFB at normoxic or hypoxic conditions. Several studies reported elevated ROS levels in keloids, indicating the increased oxidative stress. In line with previous studies, increased ROS was detected in KFB compared to NFB under normoxia. A report by Vincent [12] showed decreased ROS in keloids. The inconsistent results showed that KFB underwent regulation of

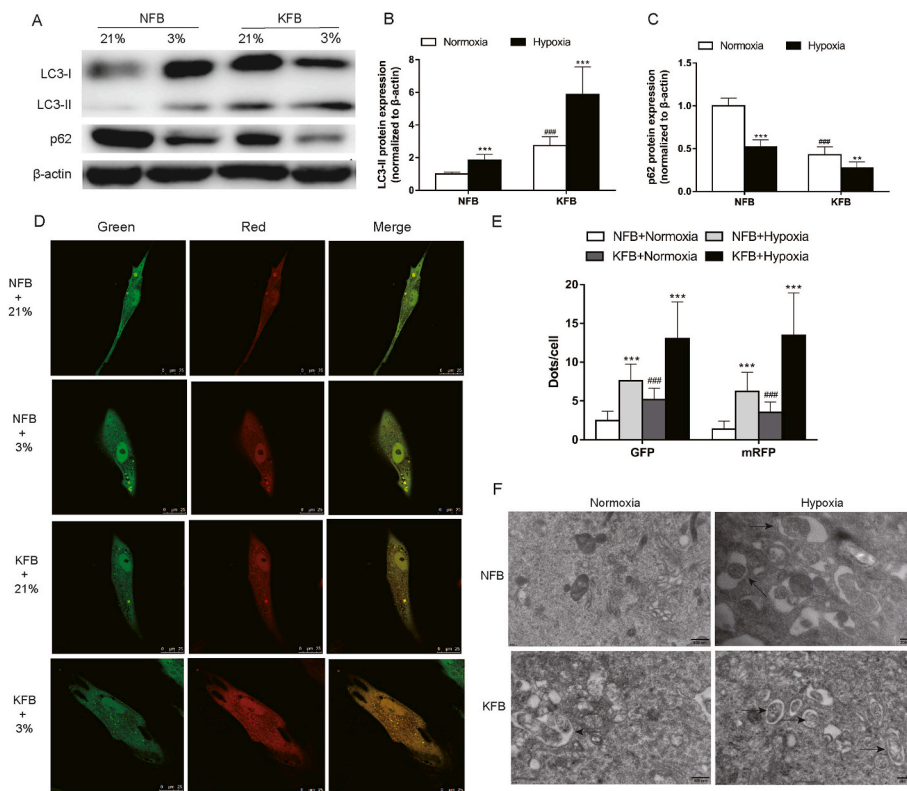


Fig. 7. Hypoxia (3%) induced autophagy in KFB and NFB. Western blotting (A) and quantification analysis (B–C) of LC3 and p62 performed after cells were conditioned at 3% O₂ for 24 h. β-actin was used as an internal standard for protein loading. (D–E) Confocal microscopy was employed to observe the formation of autophagosomes and autolysosomes through transfecting with fluorescent mRFP-GFP-LC3. (F) Electron microscopy revealed an increased number of autophagic vacuoles in KFB and NFB after incubated under hypoxia (3%) for 24 h compared with normoxia. Data are presented as Mean ± S.D. (n = 6). #P < 0.05, ##P < 0.01, ###P < 0.001 versus NFB under normoxia. *P < 0.05, **P < 0.01, ***P < 0.001 versus represent NFB or KFB in hypoxia versus that under normoxic conditions.

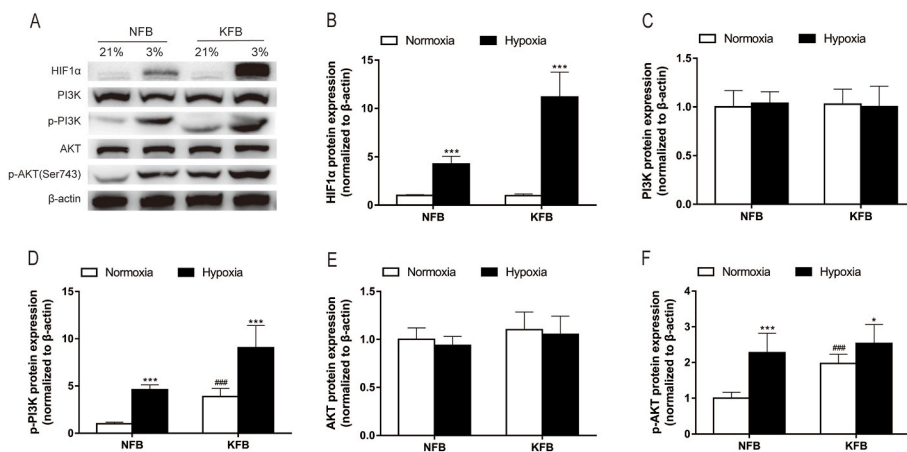


Fig. 8. HIF-1α and the PI3K-AKT pathway were upregulated in KFB and NFB under hypoxia (3%). Hypoxia (3%) for 24 h promoted upregulation of HIF-1α protein level analyzed by Western blot (A–B). (C–F) The protein levels of PI3K-AKT pathway were evaluated by western blotting after cells were cultured under hypoxia (3%) for 24 h. Hypoxia promoted the phosphorylation levels of PI3K and AKT. Data are presented as Mean ± S.D. (n = 6). #P < 0.05, ##P < 0.01, ###P < 0.001 versus NFB under normoxia. *P < 0.05, **P < 0.01, ***P < 0.001 versus represent NFB or KFB in hypoxia versus that under normoxic conditions.

oxidative stress, which was a complex balancing process. Increased mitoROS was also observed in KFB under normoxia, suggesting that more impaired mitochondria exist in keloids and electrons escape from the electron transport chain (ETC). When cells suffer from reduced O₂ availability, electrons escape from the ETC at an elevated rate and interact with O₂ prior to complex IV, resulting in superoxide anion radicals (O₂ •-). Furthermore, to maintain redox homeostasis under hypoxic condition, antioxidant activities increased. A growing body of data revealed that ROS level increased in cells exposed to hypoxia [30, 31], while other researchers detected the opposite result. For instance, Sgarbi et al. found decreased ROS levels in skin human fibroblasts and osteosarcoma 143 B cells exposed to hypoxia (0.5% O₂) [32]. Oxygen levels account for the conflicting results. O₂ serves as substrate in the formation of superoxide anion radicals. Hence, an extremely low oxygen level (0.5% O₂) would not augment ROS generation.

Previous works [14,15] suggested altered metabolism in keloids and

KFB, but the metabolic status of KFB under hypoxia remains to be investigated. In the present study, we explored the glycolysis and mitochondrial function of KFB in hypoxic condition. Annette et al. [12] reported KFB presented similar bioenergetics to cancer cells with ATP generation primarily from glycolysis as demonstrated by enhanced lactate production. Our results showed increased glucose intake and lactate production in KFB compared to NFB under normoxia. Additionally, when cells were treated with hypoxia, enhanced glucose consumption and lactate accumulation were observed in KFB and NFB. GLUT1 and LDHA expression at mRNA and protein levels also increased. HK2, PFKFB3, PGK1, ENO1 and PKM2 are crucial enzymes in glycolysis and their upregulation is tightly related to the proliferation, invasion and apoptosis of cancer cells [33,34]. In the study, we assessed the mRNA and protein expressions as well as enzyme activities of the above enzymes in KFB and NFB under hypoxic condition. Interestingly, we found that hypoxia exerted a positive effect on the expression and

activity of the investigated enzymes. Although glycolysis is considered a less efficient way to provide energy than oxidative phosphorylation, the enhanced glycolysis induced by hypoxia can rapidly provide ATP and mass intermediates for cell proliferation. Extensive studies have suggested the augmented expression of glycolytic enzymes induced by hypoxia leads to changes in malignant tumor metabolism and contributes to the proliferation, survival, EMT, invasion, apoptosis and angiogenesis of cancer cells [33–35].

Mitochondria in cancer cells are structurally and functionally distinguished from those in normal cells and participate actively in metabolic reprogramming. Hypoxia triggers specific mechanisms to adapt cells to a low O₂ microenvironment. In response to hypoxia, mitochondria undergo changes in number, fractures and functions, and adjust their metabolism. In the present study, we assessed mitochondrial mass and membrane potential in KFB and NFB under hypoxia. Strikingly, we detected an increase in mitochondrial mass and membrane potential. Traditionally, it is generally accepted that hypoxia reduces mitochondrial mass in that cancer cells resort to glycolysis instead of oxidative phosphorylation for ATP generation in hypoxic conditions [36]. A decrease in mitochondrial membrane potential indicates cells in the early stage of apoptosis. In our study, the elevated membrane potential suggested that cells were protected against apoptosis. Additionally, we observed increased abnormal mitochondria in KFB under normoxia. The impaired mitochondria exhibited swelling, vacuolization, and cristae degeneration under TEM. Abnormalities of mitochondrial morphology are tightly related to mitochondrial dysfunctions. Accordingly, the increase in mitochondrial mass and membrane potential serves as a response to decreased mitochondrial activities. The electron transport chain (ETC) is mainly comprised of mitochondrial complexes I-IV that can obviously affect the OXPHOS level and ROS production [37]. In this study, we investigated the activities of mitochondrial complexes I-IV in KFB and NFB. We found that their activities decreased in KFB compared with NFB under normoxia. Furthermore, activities of mitochondrial complexes were attenuated when cells were incubated in hypoxic condition. The healthy condition of mitochondrial complexes is closely related to ROS generation. Hence, ROS production increased in response to the impaired mitochondrial complexes caused by hypoxia.

Glycolysis and oxidative phosphorylation are the two major pathways for energy production in the cell. A majority of cells can switch between these two pathways, thereby adapting to changes in their environment [38]. To profoundly understand the effect of hypoxia on glycolysis and oxidative phosphorylation in KFB, we evaluated ECAR and OCR with a Seahorse XFp Real-time Extracellular Flux Analyzer in real time. In normoxic condition when compared to NFB, KFB exhibited higher key parameters of glycolytic flux: glycolysis, glycolytic capacity, glycolytic reserve, and nonglycolytic acidification and attenuated important parameters of mitochondrial functions including ATP production, maximal respiration, spare respiratory capacity, non-mitochondrial respiration and coupling efficiency. Furthermore, the ratio of OCR/ECAR significantly decreased in KFB in normoxia, indicating the metabolic shift to aerobic glycolysis. When treated with hypoxia, KFB and NFB presented enhanced glycolysis, glycolytic capacity and nonglycolytic acidification, and decreased glycolytic reserve. Additionally, H⁺ leak in mitochondria increased, while other key parameters of OCR were hindered by hypoxia. In addition, hypoxia suppressed OCR/ECAR in KFB and NFB, suggesting that cells undergo metabolic programming in hypoxia. These results collectively indicate that hypoxia elevates glycolysis and compromises mitochondrial functions in KFB. Moreover, apart from certain parameters such as glycolytic capacity and basal respiration with a extremely high or low baseline, KFB response to hypoxia more actively than NFB in term of most metabolic parameters.

Autophagy is crucial for maintaining cell homeostasis and survival in response to various stressful conditions [39]. The generated decomposition products are inputs to cellular metabolism, through which they

are utilized to generate energy. In addition, metabolism can reversely regulate autophagy. Qian et al. reported that the protein kinase activity of the glycolytic enzyme PGK1 regulates autophagy to promote tumorigenesis [40]. In the present study, we investigated the autophagy level in KFB and NFB. In the presence of normal oxygen, the LC3 II level in KFB is higher than that in NFB, indicating increased autophagy. What's more, increased autophagosomes and autolysosomes were observed in KFB, investigated by confocal microscopy and electron microscopy. Collectively, the autophagy in KFB was higher than that in NFB under normoxia. In the context of limited oxygen (3%), KFB and NFB exhibited enhanced LC3 II expression, and increased autophagosomes and autolysosomes, which suggested that hypoxia exerted a positive role in autophagy.

Finally, we explored the potential mechanism by which hypoxia regulates energy metabolism. HIF1 α plays a central role in cellular metabolism in response to hypoxia [41]. The PI3K/AKT pathway is upregulated in hypoxia and the signaling network has diverse downstream effects on cellular metabolism through either the control of nutrient transporters and metabolic enzymes or the regulation of key components of metabolic pathways [42]. Consequently, we determined the levels of HIF1 α and the PI3K/AKT pathway in KFB under hypoxia. In line with previous studies [43,44], we detected that HIF1 α expression and the phosphorylation of PI3K/AKT were enhanced by hypoxia. In our further study, we will investigate whether the regulation of HIF1 α and the PI3K/AKT pathway can alter metabolism in KFB under hypoxia.

Cell functions are remarkably regulated by metabolic programming. Glycolysis is closely related to the development and growth of cancers. Amparo et al. reported that aerobic glycolysis can be enhanced by HK2 and promotes tumor growth in human glioblastoma multiforme [45]. Sun and his colleagues found that oxidized ATM-mediated glycolysis enhancement in breast cancer-associated fibroblasts contributes to tumor invasion [46]. Studies on cancer treatments by glycolytic regulation are widely reported. Our preliminary work showed that the glycolytic inhibitor, 2-deoxyglucose (2-DG), suppressed the proliferation of KFB in a dose-dependent and time-dependent manner [14]. A study by Professor Li suggested that blocking glycolysis by targeting PFKFB3 inhibits tumor growth and metastasis in head and neck squamous cell carcinoma [47]. Mass efforts have focused on therapeutic targeting of glycolysis, while drugging OXPHOS has remained largely unexplored. Mitochondria are regarded as important pharmacological targets because of their key role in cellular proliferation and apoptosis. Treatment with IACS-010759, an inhibitor of complex I, robustly inhibited proliferation and induced apoptosis in models of brain cancer and acute myeloid leukemia (AML) reliant on OXPHOS [48]. Additionally, Hirpara et al. reported that an OXPHOS inhibitor, OPB-51602, exerted potent antitumorigenic effects and highlighted the potential of OXPHOS targeting strategies in therapy-resistant oncogene-addicted tumors [49]. Hence, targeting glycolysis or OXPHOS to regulating metabolism may be a potential therapy for keloid treatments.

We are aware that the lack of a keloid animal model limits our understanding of the impact of hypoxia on metabolism in vivo. Furthermore, the absence of strict matching for body sites may be a factor that affects cell phenotype. It remains to be clarified in future studies whether metabolism modulators are efficient in regulating KFB proliferation, apoptosis and ECM deposition. This needs further investigation.

In summary, we demonstrated enhanced glycolysis and compromised mitochondrial functions under hypoxia and that the HIF1 α and PI3K/AKT pathways are implicated in regulating metabolism. Although ROS generation increased, cells remained in redox homeostasis under hypoxia (3%). Additionally, autophagy was increased by hypoxia. Our findings improve the current understanding of the pathological mechanism in keloids. Strategies targeting metabolic programming triggered by hypoxia appear to be promising in the development of novel and effective keloid therapeutics.

Declaration of competing interest

The authors declared that they have no conflicts of interest to this work. We declare that we do not have any commercial or associative interest that represents a conflict of interest in connection with the work submitted.

Acknowledgments

This work was funded by National Natural Science Foundation of China (81772090).

Appendix A. Supplementary data

Supplementary data to this article can be found online at <https://doi.org/10.1016/j.redox.2020.101815>.

References

- [1] T. Liu, X. Ma, T. Ouyang, H. Chen, Y. Xiao, Y. Huang, J. Liu, M. Xu, Efficacy of 5-aminolevulinic acid-based photodynamic therapy against keloid compromised by downregulation of SIRT1-SIRT3-SOD2-mROS dependent autophagy pathway, *Redox Biology* 20 (2019) 195–203, 1.
- [2] C. Huang, L. Liu, Z. You, Y. Du, R. Ogawa, Managing keloid scars: from radiation therapy to actual and potential drug deliveries, *Int. Wound J.* 16 (2019) 852–859, 1.
- [3] Y. Chen, Q. Jin, X. Fu, J. Qiao, F. Niu, Connection between T regulatory cell enrichment and collagen deposition in keloid, *Exp. Cell Res.* 383 (2019) 111549, 1.
- [4] J.C. Smith, B.E. Boone, S.R. Opalenik, S.M. Williams, S.B. Russell, Gene profiling of keloid fibroblasts shows altered expression in multiple fibrosis-associated pathways, *J. Invest. Dermatol.* 128 (2008) 1298–1310, 1.
- [5] M. Fujita, Y. Yamamoto, J.J. Jiang, T. Atsumi, Y. Tanaka, T. Ohki, N. Murao, E. Funayama, T. Hayashi, M. Osawa, T. Maeda, D. Kamimura, M. Murakami, NEDD4 is involved in inflammation development during keloid formation, *J. Invest. Dermatol.* 139 (2019) 333–341, 1.
- [6] M.V. Libertini, J.W. Locasale, The Warburg effect: how does it benefit cancer cells? *Trends Biochem. Sci.* 41 (2016) 211–218, 1.
- [7] K. Singer, M. Kastenberger, E. Gottfried, C.G. Hammerschmied, M. Buttner, M. Aigner, B. Seliger, B. Walter, H. Schlosser, A. Hartmann, R. Andreesen, A. Mackensen, M. Kreutz, Warburg phenotype in renal cell carcinoma: high expression of glucose-transporter 1 (GLUT-1) correlates with low CD8(+) T-cell infiltration in the tumor, *Int. J. Canc.* 128 (2011) 2085–2095, 1.
- [8] E.M. Palsson-McDermott, A.M. Curtis, G. Goel, M. Lauterbach, F.J. Sheedy, L. E. Gleeson, M. van den Bosch, S.R. Quinn, R. Domingo-Fernandez, D. Johnston, J. K. Jiang, W.J. Israelsen, J. Keane, C. Thomas, C. Clish, H.M. Vander, R.J. Xavier, L. O'Neill, Pyruvate kinase M2 regulates hif-1alpha activity and IL-1 beta induction and is a critical determinant of the Warburg effect in LPS-activated macrophages, *Cell Metabol.* 21 (2015) 347, 1.
- [9] S. Dabral, C. Muecke, C. Valasarajan, M. Schmoranz, A. Wietelmann, G. L. Semenza, M. Meister, T. Muley, T. Seeger-Nukpezah, C. Samakovlis, N. Weissmann, F. Grimminger, W. Seeger, R. Savai, S.S. Pullamsetti, A RASSF1A-HIF1alpha loop drives Warburg effect in cancer and pulmonary hypertension, *Nat. Commun.* 10 (2019) 2130, 1.
- [10] L. Yang, M. Xie, M. Yang, Y. Yu, S. Zhu, W. Hou, R. Kang, M.T. Lotze, T.R. Billiar, H. Wang, L. Cao, D. Tang, PKM2 regulates the Warburg effect and promotes HMGB1 release in sepsis, *Nat. Commun.* 5 (2014) 4436, 1.
- [11] H. Wen, J.P. Ting, L.A. O'Neill, A role for the NLRP3 inflammasome in metabolic diseases—did Warburg miss inflammation? *Nat. Immunol.* 13 (2012) 352–357, 1.
- [12] A.S. Vincent, T.T. Phan, A. Mukhopadhyay, H.Y. Lim, B. Halliwell, K.P. Wong, Human skin keloid fibroblasts display bioenergetics of cancer cells, *J. Invest. Dermatol.* 128 (2008) 702–709, 1.
- [13] R. Vinaik, D. Barayan, C. Auger, A. Abdullahi, M.G. Jeschke, Regulation of glycolysis and the Warburg effect in wound healing, *JCI Insight* 5 (2020) 1.
- [14] Q. Li, Z. Qin, F. Nie, H. Bi, R. Zhao, B. Pan, J. Ma, X. Xie, Metabolic reprogramming in keloid fibroblasts: aerobic glycolysis and a novel therapeutic strategy, *Biochem. Biophys. Res. Commun.* 496 (2018) 641–647, 1.
- [15] Q. Li, Z. Qin, B. Chen, Y. An, F. Nie, X. Yang, B. Pan, H. Bi, Mitochondrial dysfunction and morphological abnormality in keloid fibroblasts, *Adv. Wound Care* 9 (2020) 539–552, 1.
- [16] R. Okuno, Y. Ito, N. Eid, Y. Otsuki, Y. Kondo, K. Ueda, Upregulation of autophagy and glycolysis markers in keloid hypoxic-zone fibroblasts: morphological characteristics and implications, *Histol. Histopathol.* 33 (2018) 1075–1087, 1.
- [17] Z. Zhang, F. Nie, C. Kang, B. Chen, Z. Qin, J. Ma, Y. Ma, X. Zhao, Increased periostin expression affects the proliferation, collagen synthesis, migration and invasion of keloid fibroblasts under hypoxic conditions, *Int. J. Mol. Med.* 34 (2014) 253–261, 1.
- [18] J. Kim, B. Kim, S.M. Kim, C.E. Yang, S.Y. Song, W.J. Lee, J.H. Lee, Hypoxia-induced epithelial-to-mesenchymal transition mediates fibroblast abnormalities via ERK activation in cutaneous wound healing, *Int. J. Mol. Sci.* 20 (2019) 1.
- [19] R. Lei, J. Li, F. Liu, W. Li, S. Zhang, Y. Wang, X. Chu, J. Xu, HIF-1alpha promotes the keloid development through the activation of TGF-beta/Smad and TLR4/MyD88/NF-kappaB pathways, *Cell Cycle* 18 (2019) 3239–3250, 1.
- [20] S.K. Parks, Y. Cormerais, J. Pouyssegur, Hypoxia and cellular metabolism in tumour pathophysiology, *J. Physiol.* 595 (2017) 2439–2450, 1.
- [21] T.W. Al, T.P. Dale, R. Al-Jumaily, N.R. Forsyth, Hypoxia-modified cancer cell metabolism, *Front Cell Dev Biol* 7 (2019) 4, 1.
- [22] H.E. Azzouzi, S. Leptidis, P.A. Doevendans, L.J. De Windt, HypoxamiRs: regulators of cardiac hypoxia and energy metabolism, *Trends Endocrinol. Metabol.* 26 (2015) 502–508, 1.
- [23] X. He, H. Zeng, R.J. Roman, J.X. Chen, Inhibition of prolyl hydroxylases alters cell metabolism and reverses pre-existing diastolic dysfunction in mice, *Int. J. Cardiol.* 272 (2018) 281–287, 1.
- [24] V. Gopu, L. Fan, R.S. Shetty, M.R. Nagaraja, S. Shetty, Caveolin-1 scaffolding domain peptide regulates glucose metabolism in lung fibrosis, *JCI Insight* 5 (2020) 1.
- [25] V. Gopu, L. Fan, R.S. Shetty, M.R. Nagaraja, S. Shetty, Caveolin-1 scaffolding domain peptide regulates glucose metabolism in lung fibrosis, *JCI Insight* 5 (2020) 1.
- [26] L.K. Senavirathna, C. Huang, X. Yang, M.C. Munteanu, R. Sathiaselan, D. Xu, C. A. Henke, L. Liu, Hypoxia induces pulmonary fibroblast proliferation through NFAT signaling, *Sci. Rep.* 8 (2018) 2709, 1.
- [27] X. Chai, D. Sun, Q. Han, L. Yi, Y. Wu, X. Liu, Hypoxia induces pulmonary arterial fibroblast proliferation, migration, differentiation and vascular remodeling via the PI3K/Akt/p70S6K signaling pathway, *Int. J. Mol. Med.* 41 (2018) 2461–2472, 1.
- [28] D.A. Ladin, Z. Hou, D. Patel, M. McPhail, J.C. Olson, G.M. Saed, D.P. Fivenson, p53 and apoptosis alterations in keloids and keloid fibroblasts, *Wound Repair Regen.* 6 (1998) 28–37, 1.
- [29] R. Lei, J. Li, F. Liu, W. Li, S. Zhang, Y. Wang, X. Chu, J. Xu, HIF-1alpha promotes the keloid development through the activation of TGF-beta/Smad and TLR4/MyD88/NF-kappaB pathways, *Cell Cycle* 18 (2019) 3239–3250, 1.
- [30] G.Y. Liou, P. Storz, Reactive oxygen species in cancer, *Free Radic. Res.* 44 (2010) 479–496, 1.
- [31] U.S. Srinivas, B. Tan, B.A. Velayappan, A.D. Jeyasekharan, ROS and the DNA damage response in cancer, *Redox Biol* 25 (2019) 101084, 1.
- [32] G. Sgarbi, G. Gorini, F. Liuzzi, G. Solaini, A. Baracca, Hypoxia and IF1 expression promote ROS decrease in cancer cells, *Cells* 7 (2018) 1.
- [33] Y. Zhang, H. Cai, Y. Liao, Y. Zhu, F. Wang, J. Hou, Activation of PGK1 under hypoxic conditions promotes glycolysis and increases stem celllike properties and the epithelial-mesenchymal transition in oral squamous cell carcinoma cells via the AKT signalling pathway, *Int. J. Oncol.* 57 (2020) 743–755, 1.
- [34] N. Azoitei, A. Becher, K. Steinestel, A. Rouhi, K. Diepold, F. Genze, T. Simmet, T. Seufferlein, PKM2 promotes tumor angiogenesis by regulating HIF-1alpha through NF-kappaB activation, *Mol. Canc.* 15 (2016) 3, 1.
- [35] W. Wan, K. Peng, M. Li, L. Qin, Z. Tong, J. Yan, B. Shen, C. Yu, Histone demethylase JMJD1A promotes urinary bladder cancer progression by enhancing glycolysis through coactivation of hypoxia inducible factor 1alpha, *Oncogene* 36 (2017) 3868–3877, 1.
- [36] D.C. Fuhrmann, B. Brune, Mitochondrial composition and function under the control of hypoxia, *Redox Biol* 12 (2017) 208–215, 1.
- [37] R.D. Guzy, B. Hoyos, E. Robin, H. Chen, L. Liu, K.D. Mansfield, M.C. Simon, U. Hammerling, P.T. Schumacker, Mitochondrial complex III is required for hypoxia-induced ROS production and cellular oxygen sensing, *Cell Metabol.* 1 (2005) 401–408, 1.
- [38] C. Jose, N. Bellance, R. Rossignol, Choosing between glycolysis and oxidative phosphorylation: a tumor's dilemma? *Biochim. Biophys. Acta* 1807 (2011) 552–561, 1.
- [39] A.V. Onorati, M. Dyczynski, R. Ojha, R.K. Amaravadi, Targeting autophagy in cancer, *Cancer* 124 (2018) 3307–3318, 1.
- [40] X. Qian, X. Li, Z. Lu, Protein kinase activity of the glycolytic enzyme PGK1 regulates autophagy to promote tumorigenesis, *Autophagy* 13 (2017) 1246–1247, 1.
- [41] K. Chen, J. Zeng, H. Xiao, C. Huang, J. Hu, W. Yao, G. Yu, W. Xiao, H. Xu, Z. Ye, Regulation of glucose metabolism by p62/SQSTM1 through HIF1alpha, *J. Cell Sci.* 129 (2016) 817–830, 1.
- [42] G. Hoxhaj, B.D. Manning, The PI3K-AKT network at the interface of oncogenic signalling and cancer metabolism, *Nat. Rev. Canc.* 20 (2020) 74–88, 1.
- [43] C.P. Cui, C.C. Wong, A.K. Kai, D.W. Ho, E.Y. Lau, Y.M. Tsui, L.K. Chan, T. Cheung, K.S. Chok, A. Chan, R.C. Lo, J.M. Lee, T.K. Lee, I. Ng, SENP1 promotes hypoxia-induced cancer stemness by HIF-1alpha deSUMOylation and SENP1/HIF-1alpha positive feedback loop, *Gut* 66 (2017) 2149–2159, 1.
- [44] C. Dou, Z. Zhou, Q. Xu, Z. Liu, Y. Zeng, Y. Wang, Q. Li, L. Wang, W. Yang, Q. Liu, K. Tu, Hypoxia-induced TUFT1 promotes the growth and metastasis of hepatocellular carcinoma by activating the Ca(2+)/PI3K/AKT pathway, *Oncogene* 38 (2019) 1239–1255, 1.
- [45] A. Wolf, S. Agnihotri, J. Micallef, J. Mukherjee, N. Sabha, R. Cairns, C. Hawkins, A. Guha, Hexokinase 2 is a key mediator of aerobic glycolysis and promotes tumor growth in human glioblastoma multiforme, *J. Exp. Med.* 208 (2011) 313–326, 1.
- [46] K. Sun, S. Tang, Y. Hou, L. Xi, Y. Chen, J. Yin, M. Peng, M. Zhao, X. Cui, M. Liu, Oxidized ATM-mediated glycolysis enhancement in breast cancer-associated fibroblasts contributes to tumor invasion through lactate as metabolic coupling, *EBioMedicine* 41 (2019) 370–383, 1.
- [47] H.M. Li, J.G. Yang, Z.J. Liu, W.M. Wang, Z.L. Yu, J.G. Ren, G. Chen, W. Zhang, J. Jia, Blockage of glycolysis by targeting PFKFB3 suppresses tumor growth and

- metastasis in head and neck squamous cell carcinoma, *J. Exp. Clin. Oncol.* 36 (2017) 7, 1.
- [48] J.R. Molina, Y. Sun, M. Protopopova, S. Gera, M. Bandi, C. Bristow, T. McAfoos, P. Morlacchi, J. Ackroyd, A.A. Agip, G. Al-Atrash, J. Asara, J. Bardenhagen, C. Carrillo, C. Carroll, E. Chang, S. Ciurea, J.B. Cross, B. Czako, A. Deem, N. Daver, J.F. de Groot, J.W. Dong, N. Feng, G. Gao, J. Gay, M.G. Do, J. Greer, V. Giuliani, J. Han, L. Han, V.K. Henry, J. Hirst, S. Huang, Y. Jiang, Z. Kang, T. Khor, S. Konoplev, Y.H. Lin, G. Liu, A. Lodi, T. Lofton, H. Ma, M. Mahendra, P. Matre, R. Mullinax, M. Peoples, A. Petrocchi, J. Rodriguez-Canale, R. Serreli, T. Shi, M. Smith, Y. Tabe, J. Theroff, S. Tiziani, Q. Xu, Q. Zhang, F. Muller, R.A. DePinho, C. Toniatti, G.F. Draetta, T.P. Heffernan, M. Konopleva, P. Jones, M.E. Di Francesco, J.R. Marszalek, An inhibitor of oxidative phosphorylation exploits cancer vulnerability, *Nat. Med.* 24 (2018) 1036–1046, 1.
- [49] J. Hirpara, J.Q. Eu, J. Tan, A.L. Wong, M.V. Clement, L.R. Kong, N. Ohi, T. Tsunoda, J. Qu, B.C. Goh, S. Pervaiz, Metabolic reprogramming of oncogene-addicted cancer cells to OXPHOS as a mechanism of drug resistance, *Redox Biol* 25 (2019) 101076, 1.